9. Panda, S. P., Kulkarni, S. G., Kakade, S. D., Tiwari, S. P. and Rao, K. P., On performance evaluation of a new liquid propellant. *Def. Sci. J.*, 1986, **36**, 1–8.
10. Kulkarni, S. G., Bagalkote, V. S., Sharawati, S., Patil, U., Pramodh Kumar and Anil Kumar, V., Theoretical evaluation and experimental validation of performance parameters of new hypergolic liquid fuel blends with red fuming nitric acid as oxidizer. *Propell. Explos. Pyrotech.*, 2009, **34**, 520–525.
11. Salem, M. Z. M., Ali, H. M. and Basalah, M. O., Essential oils from wood, bark, and needles of *Pinus roxburghii* Sarg, from Alexandria, Egypt: antibacterial and antioxidant activities. *BioResources*, 2014, **9**, 7454–7466.
12. Saei-Dehkordi, S. S., Khalighi-Sigaroodi, F., Pirali-Kheirabadi, K., Saei-Dehkordi, S. S., Alimardani-Naghani, F. and Fallah, A. A., Chemical composition, antioxidative capacity and antimicrobial activity of *Zeravschania membranacea* (Boiss.) Pimenov essential oil. *J. Food Saf.*, 2014, **34**, 87–94.
13. Nagaboopathy, M., Vijayanand, C., Hegde, G., Reddy, K. P. J. and Arunan, E., Single pulse shock tube for ignition delay studies. *Curr. Sci.*, 2008, **95**, 78–82.
14. Sharath, N., Reddy, K. P. J. and Arunan, E., Thermal decomposition of propargyl alcohol: single pulse shock tube experimental and *ab initio* theoretical study. *J. Phys. Chem. A*, 2014, **118**, 5927–5938.
15. Vasu, S. S., Davidson, D. F. and Hanson, R. K., Jet fuel ignition delay times and modeling: studies at high pressures and low temperatures in a shock tube. In 43rd AIAA/ASME/SAE/ASEE Joint Propulsion Conference and Exhibit, Cincinnati, OH, Paper AIAA-2007-5671, 8–11 July 2007.
16. Qin, Z., Yang, H. and Gardiner Jr, W. C., Measurement and modeling of shock-tube ignition delay for propene. *Combust. Flame*, 2001, **124**, 246–254.
17. Healy, D., Donat, N. S., Aul, C. J., Petersen, E. L., Zinner, C. M., Bourque, G. and Curran, H. J., *n*-Butane: ignition delay measurements at high pressure and detailed chemical kinetic simulations. *Combust. Flame*, 2010, **157**, 1526–1539.
18. Pang, G. A., Davidson, D. F. and Hanson, R. K., Experimental study and modeling of shock tube ignition delay times for hydrogen–oxygen–argon mixtures at low temperatures. *Proc. Combust. Inst.*, 2009, **32**, 181–188.
19. Hong, Z., Pang, G. A., Vasu, S. S., Davidson, D. F. and Hanson, R. K., The use of driver inserts to reduce non-ideal pressure variations behind reflected shock waves. *Shock Waves*, 2009, **19**, 113–123.
20. Ryan, T. W., Schwab, S. T. and Harlowe, W., Aluminium alkyl derivatives – ignition and combustion enhancers for supersonic combustors. *J. Propul. Power*, 1995, **11**, 124–129.

ACKNOWLEDGEMENTS. We thank IISc–ISRO Space Technology Cell, Defence Research and Development Laboratory, Defence Research and Development Organization, and Aeronautics Research and Development Board for financial support.

Received 21 October 2014; revised accepted 26 January 2015

Comparison of performance of solar photovoltaics on dual axis tracker with fixed axis at 13°N latitude

Roshan R. Rao, H. R. Swetha, J. Srinivasan and Sheela K. Ramasesha*

Divecha Centre for Climate Change, Indian Institute of Science, Bengaluru 560 012, India

Tracking systems, that continually orient photovoltaic (PV) panels towards the Sun, are expected to increase the power output from the PV panels. Tremendous amount of research is being done and funds are being spent in order to increase the efficiency of PV cells to generate more power. We report the performance of two almost identical PV systems; one at a fixed latitude tilt and the other on a two-axis tracker. We observed that the fixed axis PV panels generated 336.3 kWh, and the dual-axis Sun-tracked PV panels generated 407.2 kWh during August 2012–March 2013. The tracked panels generated 21.2% more electricity than the optimum tilt angle fixed-axis panels. The cost payback calculations indicate that the additional cost of the tracker can be recovered in 450 days.

Keywords: Cost payback time, dual axis Sun tracker, energy conversion, solar panel.

THE annual average growth rate of solar photovoltaic (PV) operating capacity in the world was the highest at 55% during 2008 through 2013 followed by concentrated solar power at 48% and wind power at 21% (ref. 1). The amount of solar energy incident on the surface of the Earth is several times more than the global energy consumption[1]. The major source of electricity in India as of November 2014 is from thermal sources (69%), followed by nuclear and hydroelectric sources (17%) and the renewable energy sources (14%)[2]. Currently, among the renewable energy sources, wind power share is 66%, biomass and bagasse cogeneration is 12.7%, small hydro and others is 12.3% and solar energy is 9% (ref. 3). India receives an annual average global horizontal insolation (GHI) of about 5 kWh/m^2/day (ref. 2) and nearly 58% of the geographical land area has the potential for solar energy production, which translates to a solar potential of nearly 9 million GWh per day[4]. PV panels have a great potential in meeting the energy demand of the country and at the same time protecting our environment by reducing CO_2 emissions in their life cycle[5]. In this scenario, it is necessary to utilize as much solar energy as possible to generate electricity.

If the conventional flat PV panel systems with a fixed tilt angle are used, during the course of the day the sunlight incident will be along the surface in the morning

*For correspondence. (e-mail: sheela@caos.iisc.ernet.in)

and evening. Also, the seasonal change in position of the Sun has to be taken care of by changing the tilt angle of the panel to obtain maximum power all through the year. The annual optimum tilt angle has been verified by calculations to be approximately equal to the latitude of the geographical location for the Indian region[6]. The loss of energy when using the yearly average fixed angle is around 15% compared with the monthly optimum tilt[6]. This gives a strong reason to use dual-axis Sun tracker. The process of following the position of the Sun is known as Sun tracking. Use of dual-axis Sun tracking device eliminates the tilt angle modification and enables maximum power output during all seasons. Few studies in Turkey have reported that energy generation increases by 64% during May and June using a two-axis Sun tracking device[7]. Previous studies carried out in Europe, have shown that the average power output of the tracking module was 13–15% (ref. 8) and 31% (ref. 9) higher than the fixed module. This large range in power output improvement from 13% to 31% is understandable. The actual improvement depends upon the relative amount of direct and diffuse radiation. The total radiation, GHI reaching the flat surface on the ground is the sum of the direct normal irradiance (DNI) component which is the direct beam radiation and diffuse radiation component which is the radiation scattered by the atmosphere. The relative amount of direct and diffuse radiation depends upon the cloudiness and aerosols in a given location. Hence it is not possible to predict a priori the additional energy that can be generated by tracking the Sun. It is therefore essential to obtain field data.

Our experiment has been set up on the rooftop of a building on the campus of Indian Institute of Science (IISc), Bengaluru. The location of the site is 13.02°N lat. and 77.57°E long. The experimental set-up includes two sets of PV modules, each set having two 230 W polycrystalline silicon PV modules connected in series[10]. The area of each 230 W panel is 1.46 m^2. One of the sets is mounted on a Sun-tracker device and the other on a fixed stand with a tilt angle of 15° facing due south (Figure 1). The monthly mean optimum tilt angle varies widely throughout the year and if annual optimum angle tilt angle is used, there can be loss of up to 13.4% compared to using monthly mean optimum tilt angle[9]. For a fixed tilt angle in Bengaluru region, the optimum tilt angle is estimated to be between 15° and 17° (ref. 11); hence we have used 15°. The two sets of PV modules are electrically connected in parallel and fed to a grid interactive inverter which converts DC power to single-phase AC power and feeds to the local grid (Figure 2). The grid connected inverter (GCI) used is a Liebert EEU 010 unidirectional inverter, whose solar input voltage varies from 40 to 88 V and output is 230 V with 1% tolerance

Figure 1. Experimental set-up: (Right) Fixed axis panels and (left) Dual axis panels.

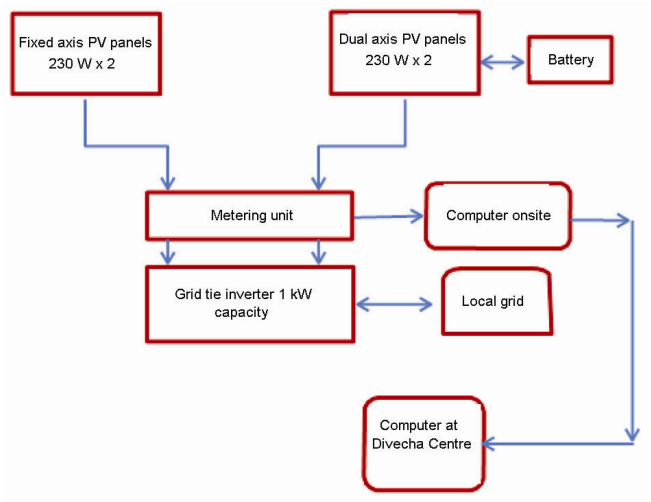

Figure 2. Block diagram of the experimental set-up, data acquisition and monitoring devices.

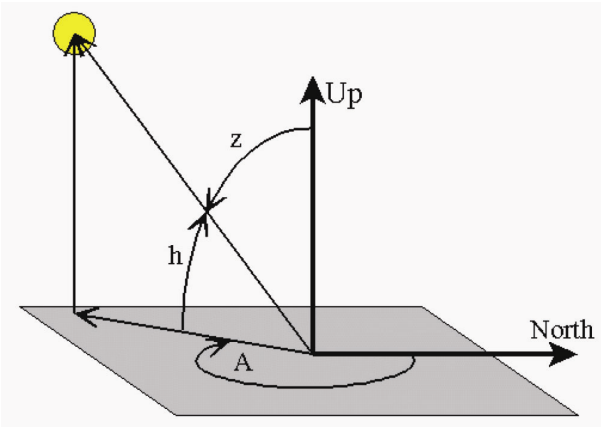

h, Elevation angle, measured up from horizon
z, Zenith angle, measured from vertical
A, Azimuth angle, measured clockwise from North

Figure 3. Solar zenith angle and solar azimuth angle which specify the position of the Sun (http://www.esrl.noaa.gov/gmd/grad/solcalc/azelzen.gif).

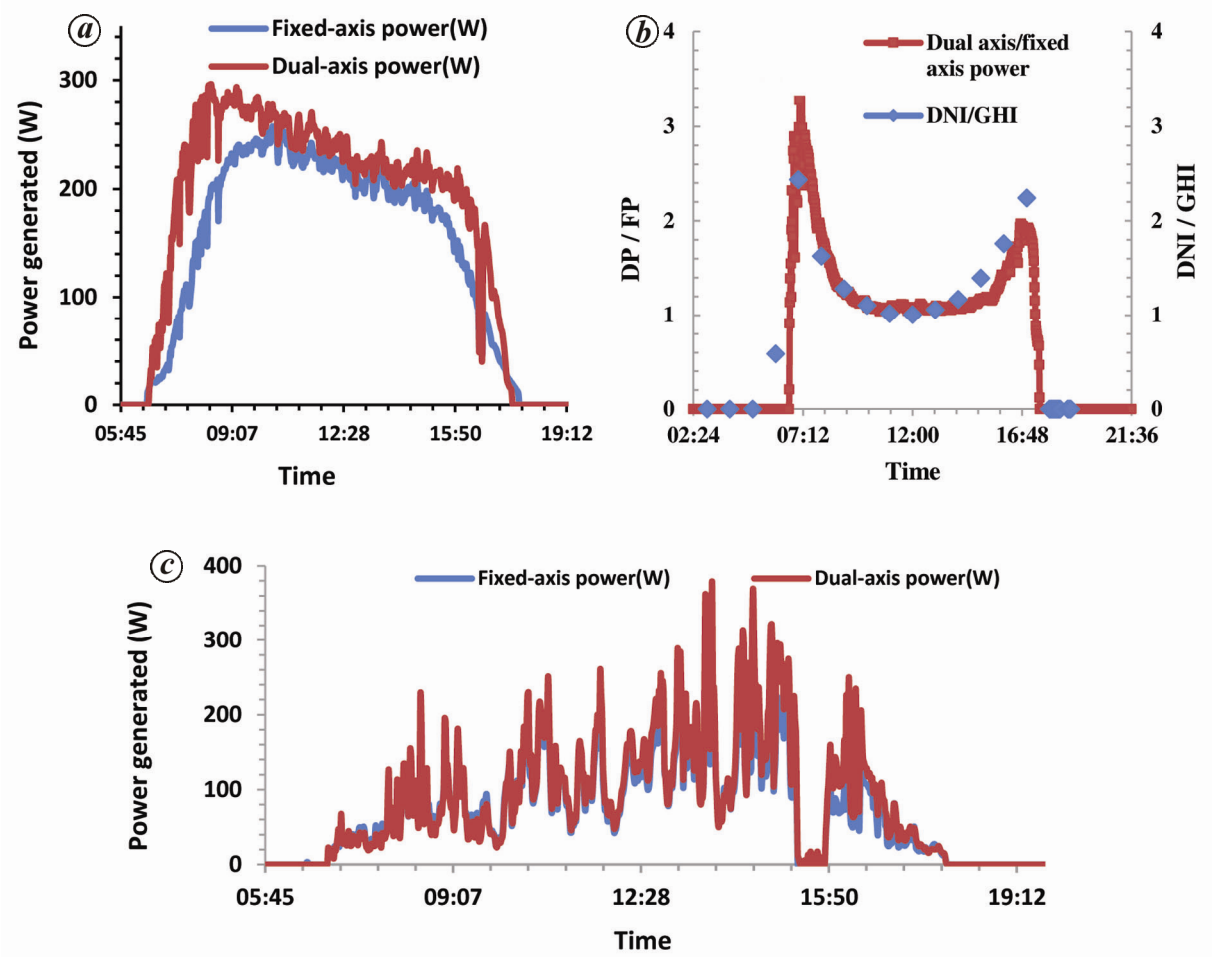

Figure 4. ***a***, Power versus time of dual axis and fixed axis panels on a clear sunny day. ***b***, Dual axis panel power/fixed axis panel power and direct normal irradiance/global horizontal insolation (GHI) versus time on a clear day. ***c***, Power versus time of dual axis and fixed axis panels on a cloudy day.

single-phase AC voltage at 50 Hz with tolerance of 3 Hz. The total input voltage fed to the inverter from each set of modules is maintained around 60 V DC and the AC output voltage from the inverter is maintained a few volts higher than the utility grid voltage to ensure that solar energy is fed and utilized by the local grid. The inverter stops feeding solar energy to the grid when there is no utility grid supply. Digital DC and AC meters are used to measure the solar DC power from the panels and AC power being fed to local grid from the GCI. The digital meters are connected to the computer using RS 232 serial communication ports. Real-time performance monitoring system has been set up and data-logging system stores the data every minute in the computer. A software interface is developed which records date/time, instantaneous DC power (in watts) generated by the fixed axis, dual axis and AC power fed to the grid every minute. Also, instantaneous cumulative DC and AC energy (kWh) are logged in. The solar radiation data have been taken from a pyranometer mounted on the rooftop and the instrument records GHI values (W/m^2) every 2 min, while DNI data are from Indian Society of Heating, Refrigerating and Air-Conditioning Engineers (ISHRAE)[12]. All the parameters calculated by us are based on the equations in IEC 61724 (ref. 13).

The dual-axis Sun tracker is a cast steel structure and its working is based upon precise algorithm for astronomical timings, which tracks the Sun continuously throughout the year. The latitude, longitude and elevation information is fed to the program at the installation time and no inputs are required during its operation time. The accuracy of the tracker claimed by the manufacturer is 0.2°. The device consumes auxiliary energy of less than 0.02 kWh and for a few seconds from a 12V 7.5 Ah battery. The device is featured with sleep mode at sunset. The Sun tracker is designed to operate with two panels on each side of the central shaft with maximum weight of 20 kg each. The panel is mounted on the tracker device with a tubular pipe structure. The Sun tracker uses the geographical position values to locate the Sun. The tracking system is independent of weather conditions and it moves the panel array according to the calculations. The

Table 1. Electrical data of the both fixed and dual axis on 25 September 2012

	Current (A)		Power (W)		Cumulative energy at the end of the hour (kWh)	
Hour	Fixed-axis	Dual axis	Fixed axis	Dual axis	Fixed axis	Dual axis
6:00 AM	0.346254	0.694028	20.4	40.4	0.011329	0.022985
7:00 AM	1.28541	3.073438	75.8	179.1	0.100906	0.232776
8:00 AM	3.151601	4.689546	186.9	275.1	0.317454	0.549499
9:00 AM	3.964438	4.709336	236.2	277.5	0.589626	0.868485
10:00 AM	4.057258	4.407789	242	259.9	0.868196	1.167465
11:00 AM	3.857287	4.23567	230	249.6	1.132851	1.454679
12:00 PM	3.636461	3.953093	216.7	232.8	1.381597	1.721926
1:00 PM	3.442728	3.757527	205	221.1	1.617263	1.976027
2:00 PM	3.271878	3.673126	194.7	216	1.841655	2.225454
3:00 PM	2.837371	3.534338	168.8	207.8	2.035067	2.464191
4:00 PM	1.602007	2.609042	95.23	153.3	2.143108	2.638933
5:00 PM	0.51452	0.718377	30.5	42.1	2.169818	2.675192
6:00 PM	0	0	0	0	2.169818	2.675192

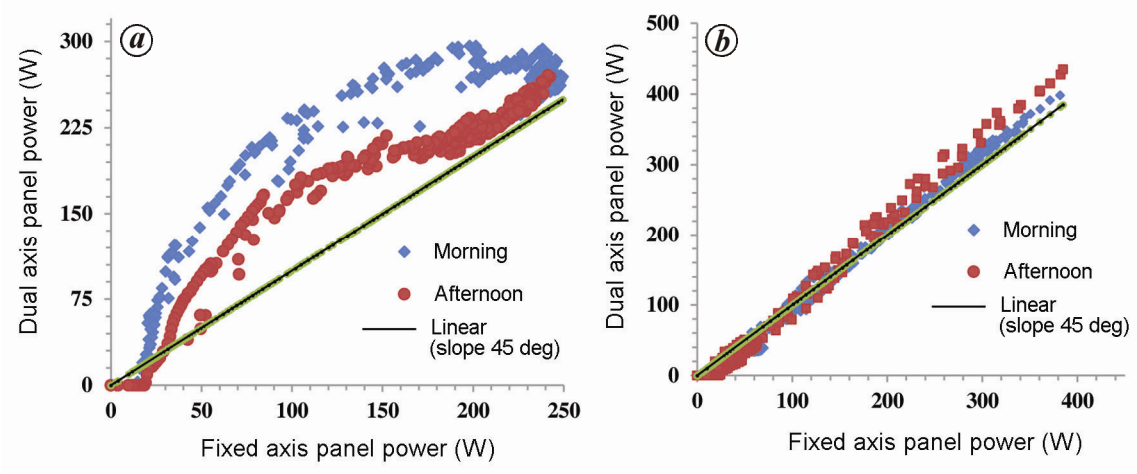

Figure 5. Power generated by panels on dual axis versus fixed axis on (***a***) a clear day and (***b***) a cloudy day.

on-board program calculates the position of the Sun every 18 sec and controls the motors, which enables the panels to track the Sun. The following formulae are used by the Sun tracker to calculate the solar zenith angle (SZA) (eq. (5)) and solar azimuth angle (eq. (6))[11,14].

The fractional year g in degrees is calculated using

$$g = (360/365.25)*(N + \text{hour}/24), \quad (1)$$

where N is the day number in a year.

Hour is the local hour and it is expressed in fractions of hours.

Declination of the Sun is calculated using the formula

$$D = 0.396372 - 22.91327*\cos(g) + 4.02543*\sin(g) - 0.387205*\cos(2*g) + 0.051967*\sin(2*g) - 0.154527*\cos(3*g) + 0.084798*\sin(3*g). \quad (2)$$

Time correction

$$TC = 0.004297 + 0.107029*\cos(g) - 1.837877*\sin(g) - 0.837378*\cos(2*g) - 2.340475*\sin(2*g). \quad (3)$$

The solar hour angle (SHA)

$$SHA = (\text{Hour} - 12)*15 + \text{longitude} + TC. \quad (4)$$

The Sun zenith angle (SZA) (Figure 3) is calculated as

$$\cos(SZA) = \sin(\text{Latitude})*\sin(D) + \cos(\text{latitude})*\cos(D)*\cos(SHA). \quad (5)$$

SZA is the complementary angle of the Sun elevation angle or altitude (SEA).

The azimuth angle (AZ) (Figure 3) is calculated as follows

$$\cos(AZ) = (\sin(D) - \sin(\text{latitude})*\cos(SZA))/(\cos(\text{latitude})*\sin(SZA)). \quad (6)$$

The experiment was set up during the second week of July 2012 and after a few minor corrections, it was performed from August 2012 till March 2013.

The power generated by dual-axis and fixed-axis panels on 25 September 2012, which was a clear day, is shown

in Figure 4 *a*. The dual-axis system generates more power than the fixed-axis system in the morning and late afternoon. The improvement in the morning is higher than in the afternoon, which is due to the drop in efficiency of the panels as they get heated up during afternoon. The morning improvement is more than the evening improvement and the improvement curve follows the DNI/GHI curve as shown in Figure 4 *b*. Table 1 gives the current, power and energy-generated data recorded for both fixed and dual-axis PV panels from 6 AM to 6 PM for 25 September 2012. On a cloudy day, as shown in Figure 4 *c*, improvement in power generation by the dual-axis system is almost absent. The improvement on a bright day is over 20%. From Figure 5 *a* and *b*, it can be seen that the presence of clouds has a high impact on improvement on account of a dual-axis Sun tracker. On a clear sky, the panels on the dual-axis tracker show an improvement (Figure 5 *a*) and on a cloudy day improvement is almost absent (Figure 5 *b*). Using the 45° slope line as reference, we can see the improvement of the dual-axis panels over the fixed-axis panels. The gap is wider during a clear day indicating high improvement, while it is almost absent during a cloudy day, meaning no improvement. During a sunny day the panel gets heated up till noon and the efficiency drops afternoon, which can be seen as a hysteresis in power generated by dual-axis for increasing and decreasing fixed-axis power generation. During a cloudy day, the temperatures of the panels are lower due to cloudiness and this gives a linear relation for the fixed-axis and dual-axis power generation. In Figure 6, DC conversion efficiency of the panels is plotted as a function of module temperature for fixed axis. It is known that increase in temperature decreases the power output from the panels leading to reduction in their efficiencies[15,16], which is seen in our data too. The solar cell efficiency is calculated as the ratio of P_{max} to P_{in}, where

$$P_{max} = V_{oc} \times I_{sc} \times \mathrm{FF} = V_{mp} \times I_{mp}, \tag{7}$$

and P_{in} is the solar irradiance on the cells. V_{oc} the open circuit voltage, I_{sc} the short circuit current, V_{mp} and I_{mp} are the maximum voltage and current respectively, and FF the fill factor is

$$\mathrm{FF} = (V_{mp} \times I_{mp})/(V_{oc} \times I_{sc}), \tag{8}$$

which is a measure of the squareness of the *IV* curve. The relation between I_{sc} and V_{oc} is

$$I_{sc} = I_0 (e^{(qV_{oc}/kT)} - 1), \tag{9}$$

where I_0 is the reverse saturation current, q the electron charge, k the Boltzmann constant and T is the temperature. On differentiating, and neglecting smaller order terms, we get

$$\frac{dV_{oc}}{dT} = \frac{V_{go} - V_{oc} + \gamma\left(\frac{kT}{q}\right)}{T}, \tag{10}$$

where V_{go} is the zero temperature bandgap voltage, and γ generally takes values between 1 and 4; for silicon $\gamma = 3$. For silicon, $(dV_{oc}/dT) = \sim 2.3$ mV/°C. When the temperature increases, I_{sc} increases by a very small magnitude, but V_{oc} and FF dominantly decrease and thus efficiency drops with an increased temperature[17]. In our experiment the efficiency decreased at a rate of about 0.3%/°C in the temperature range 20–45°C.

The daily energy generated by the Sun-tracked and the fixed-axis systems for November is plotted in Figure 7 along with the daily GHI. During the middle of the month, both GHI and the energies generated are high. The energy generated on 14 November was highest from both sets of panels with total GHI of 6315 W/m^2. The energy conversion efficiency of the panels, calculated from our data, is 10–14% as against the reported value of 15.7% by the panel manufacturing company. Figure 8 shows the total DC energy generated from fixed and dual-axis panels along with the total GHI for the period August 2012 to March 2013. Because of the clouds and haze during monsoon months of August to October, power generated by the solar panels is less than that during non-monsoon months of November to March. Calculating the monthly improvement in energy generated by the dual-axis system over the fixed-axis system, it has been found that January has the highest improvement of 32.5% (Figure 9).

With the data collected from our experiment till 31 March 2013, it can be seen that the fixed-axis panels have generated 336.32 kWh and dual-axis panels have generated 407.23 kWh of DC energy. The daily mean improvement with the dual-axis panels is 21.2% compared to optimum tilt angle fixed-axis panels. The percentage benefit is much lower during the period of the study than the predicted 35% (ref. 11), which could be due to cloudy and hazy days in the monsoon season.

The power generated by fixed-axis panels is plotted against GHI for a particular day in a month for all

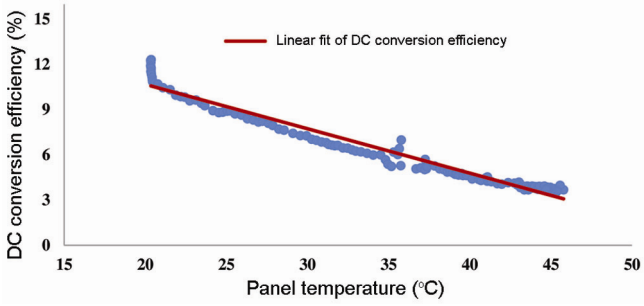

Figure 6. Plot of efficiency drop with increase in the panel temperature.

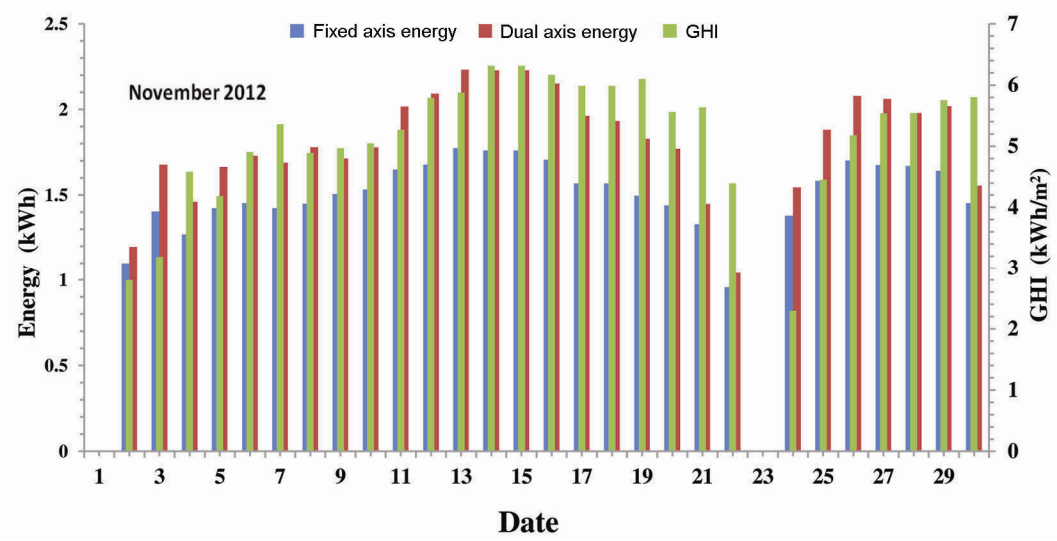

Figure 7. Daily energy generated in November 2012.

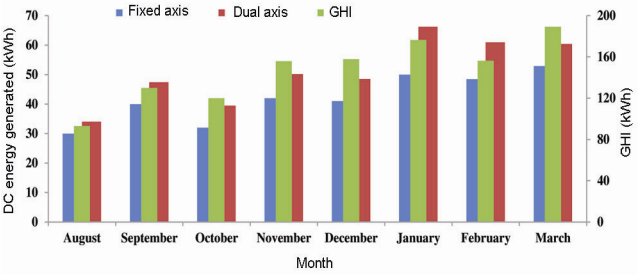

Figure 8. Energy generated by the fixed axis and dual axis systems during August 2012 to March 2013 along with the total monthly GHI.

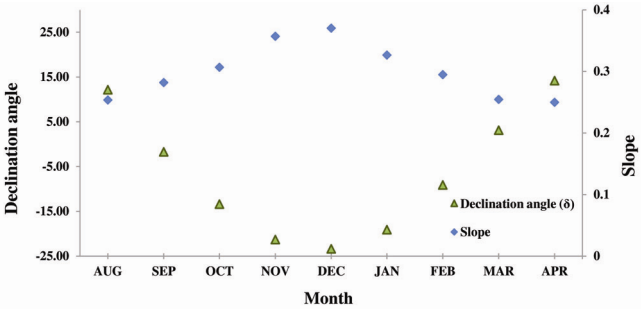

Figure 10. Plot showing variation of slope between the power generated and GHI with declination angle.

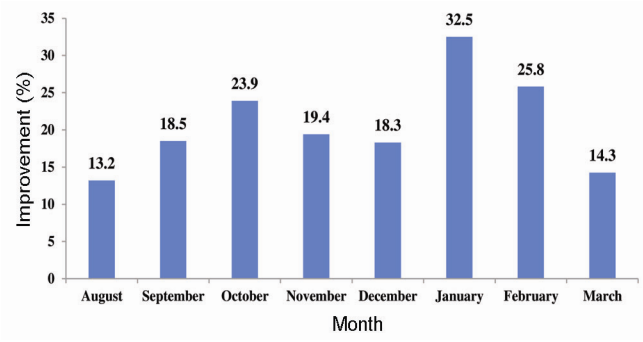

Figure 9. Monthly mean average improvement of dual axis panels over fixed axis panels.

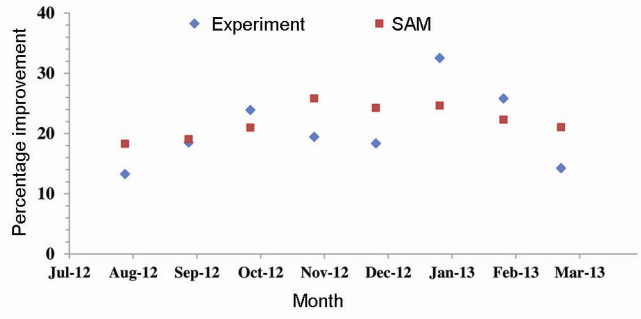

Figure 11. Results of monthly mean improvement from experiment and simulation tool.

months. The slope of this line correlates with variation of the declination angle at the location. As we can see from Figure 10, the slope is inversely proportional to the magnitude of declination angle. The slope is maximum for December and minimum for August and March. This is due to the elevation angle varying with the rotation of the Earth.

We have simulated the experiment using SAM (system advisor model) modelling tool[18]. From the modelling, we have evaluated the total energy output from fixed-axis and dual-axis PV for the period under study. The weather file is from the weather dataset published by the ISHRAE[12]. The input parameters for modelling are listed in Table 2.

The monthly energy outputs as observed in our experiment and calculated by SAM tool were compared. The calculated energy values for both dual and fixed-axis systems are higher than the experimental data. This could be

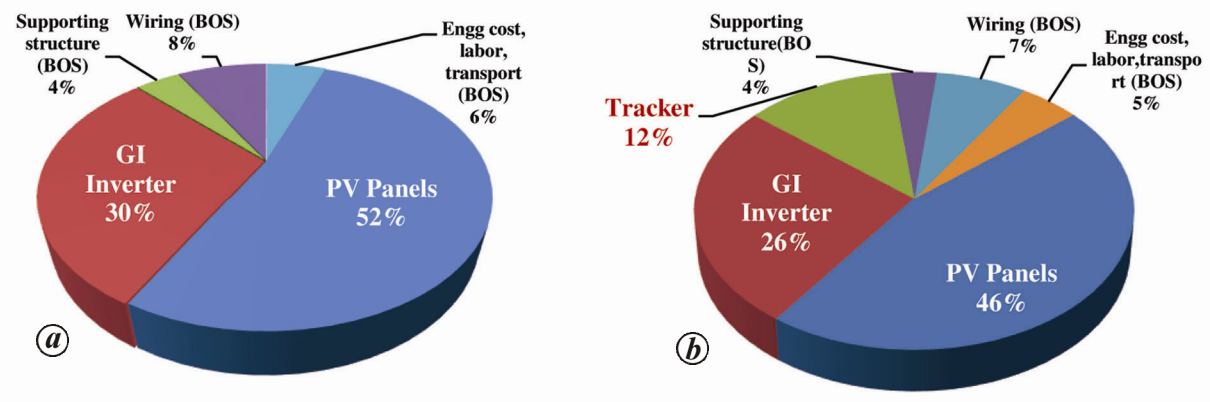

Figure 12. Cost break-up percentage for (***a***) fixed axis system cost per watt – Rs 145/W_{dc} (US$ 2.4/W_{dc}) and (***b***) with tracking device cost per watt – Rs 165/W_{dc} (US$ 2.75/W_{dc}).

Table 2. Specification of module used in the simulation

Type	Poly-Si
Nominal power	230 W
Efficiency of module	12%
Open circuit voltage	37.11 V
Short circuit current	8.18 A
Coefficient of power	–0.489%/°C

due to experimental conditions like temperature of the panels, local dust and shading on the panel part of the day.

The monthly mean improvement in the energy generated by the dual-axis system over the fixed-axis system has been calculated for the period under study. Figure 11 shows the experimental data along with those calculated from SAM. The agreement between the experimental data and the calculated data is within 8%.

Putting together the expenditure incurred (in rupees) for installing the dual-axis tracker (Figure 12), we have calculated the payback time that is required to offset the additional cost of the Sun tracker.

Our installation cost:

(1) 500 W system without tracker:
Rs 73,131 (US$ 1218.8 at Rs 60 = US$ 1).

(2) 500 W system with tracker:
Rs 93,131 (US$ 1552.2) [27.35% more than without tracker].

Assuming the feed in tariff (FiT) of Rs 12.5/unit, which was the tariff quoted during the first phase of the National Solar Mission (JNNSM)[19], the Sun tracker device cost will be paid back in around 450 days. Post 450 days, the benefit of Sun tracking system is enjoyed without any additional cost.

Thus solar PV technology is a promising source of energy for the future, but it is limited by few factors. The solar cells can produce energy only during daytime and many atmospheric conditions like clouds, aerosols, dust and temperature strongly affect power generation. The maximum attainable energy conversion efficiency depends on the solar cell materials, and is 12–20% for silicon multicrystalline cells[20]. The Sun tracker which allows for improvement in power generation during early morning and late evening requires a robust design to face the Sun at reasonable accuracy withstanding environmental factors like rain, wind, etc. As it is has moving mechanical parts and coupled electronics, it requires frequent maintenance and attendance.

From the experiments carried out by placing PV panels on a dual-axis Sun tracker and fixed-axis stand side by side, the following conclusions have been arrived at:

(a) Even during cloudy monsoon months, power could be generated from solar panels. With the fixed axis 460 Wp system, more than 100 units of DC energy was generated during the monsoon months of August to October.

(b) Temperature of the panels has a strong influence on the power generation capability of the panels studied. The power generated by the panels in the afternoon is less than that in the morning for similar GHI values.

(c) The power generated by the dual-axis tracked system is higher than the fixed-axis system in the mornings and late evenings. Over the entire period under consideration, the dual-axis panels showed a daily average improvement of 21.2%.

(d) The improvement of panels on dual axis over the fixed axis depends on cloudiness, ratio of DNI to GHI, and temperature of the modules.

(e) Cost analysis of the tracking system as against the fixed-axis system indicates that the additional cost of the tracker is recovered in 450 days, assuming FiT of Rs 12.50 per unit of electricity.

1. REN21, Renewables 2014 Global Status Report, 2014; http://www.ren21.net/REN21Activities/GlobalStatusReport.aspx

2. Executive summary, Power Sector, Central Electricity Authority, Ministry of Power, Government of India (GoI), November 2014; http://www.cea.nic.in/reports/monthly/executive_rep/nov14.pdf
3. Physical progress (achievements), Ministry of New and Renewable Energy, GoI, December 2014; http://www.mnre.gov.in/mission-and-vision-2/achievements/
4. Ramachandra, T. V., Jain, R. and Krishnadas, G., Hotspots of solar potential in India. *Renew. Sustain. Energy Rev.*, 2011, **15**, 3178–3186.
5. Briner, G., The climate change mitigation potential of the solar PV industry: a life cycle perspective. M Sc thesis, Centre for Environmental Policy, Imperial College London, September 2009.
6. Jamil Ahmad, M. and Tiwari, G. N., Optimization of tilt angle for solar collector to receive maximum radiation. *Open Renew. Energy J.*, 2009, **2**, 19–24.
7. Kivrak, S., Gunduzalp, M. and Dincer, F., Theoretical and experimental performance investigation of a two-axis solar tracker under the climatic condition of Denizli, Turkey. *PRZEGLĄD ELEKTROTECHNICZNY (Electrical Review)*, ISSN 0033-2097, R. 88 NR 2/2012.
8. Şenpinar, A. and Cebeci, M., Evaluation of power output for fixed and two-axis tracking PV arrays. *Appl. Energy*, 2012, **92**, 677–685.
9. Helwa, N. H., Bahgat, A. B. G., El Shafee, A. M. R. and El Shenawy, E. T., Maximum collectable solar energy by different solar tracking systems. *Energy Sources*, 2000, **22**, 1 and 2.
10. Solar photovoltaic module (Kotak Urja Pvt Ltd) datasheet; http://www.kotakurja.com/PhotovoltaicsModules/pdfs/230%20Wp-%20Kotak%20PV%20Data%20Sheet.pdf
11. Fahl, P. and Ganapathisubbu, S., Tracking benefits for solar collectors installed in Bangalore. *J. Renew. Sustain. Energy*, 2011, **3**(2), 023103.
12. Weather data, Asia WMO region 2: India, energy efficiency and renewable energy, US Department of Energy; http://apps1.eere.energy.gov/buildings/energyplus/cfm/weather_data3.cfm/region=2_asia_wmo_region_2/country=IND/cname=India/
13. Photovoltaic system performance monitoring – guidelines for measurement, data exchange and analysis. IEC 61724, 1998; https://law.resource.org/pub/in/bis/S05/is.iec.61724.1998.pdf
14. Duffie, J. A. and Beckman, W. A., *Solar Engineering of Thermal Processes*, Wiley, New York, 2006, 3rd edn.
15. Radziemska, E., The effect of temperature on the power drop in crystalline silicon solar cells. *Renew. Energy*, 2003, **28**(1), 1–12.
16. Meral, M. E. and Dinçer, F., A review of the factors affecting operation and efficiency of photovoltaic based electricity generation systems. *Renew. Sustain. Energy Rev.*, 2011, **15**(5), 2176–2184.
17. Green, M. A. *Solar Cells: Operating Principles, Technology, and System Applications*, Prentice-Hall, Inc., Englewood Cliffs, NJ, 1982.
18. NREL system advisor model (SAM), energy efficiency and renewable energy, US Department of Energy; https://sam.nrel.gov/
19. Jawaharlal Nehru National Solar Mission, Ministry of New and Renewable Energy, GoI, December 2012; http://mnre.gov.in/file-manager/UserFiles/draft-jnnsmpd-2.pdf
20. National Centre for Photovoltaics, NREL, US Department of Energy; http://www.nrel.gov/ncpv/images/efficiency_chart.jpg

ACKNOWLEDGEMENT. We thank Divecha Centre for Climate Change, IISc, Bengaluru for financial support.

Received 22 October 2014; revised accepted 12 February 2015

Amelioration of fluoride toxicity using amla (*Emblica officinalis*)

Sumeet Ranjan and Shahla Yasmin*

Department of Zoology, Patna Women's College, Patna 800 001, India

A study was conducted on the residents of Bhupnagar, a fluoride endemic village in Gaya district, Bihar, to assess the ameliorating effect of amla (*Emblica officinalis*) on fluoride-induced toxicity. Fifty-three subjects of different age groups were included in the study. Among these, 27 subjects (test group) were given amla powder as dietary supplement for 9 months and the rest 26 subjects were kept as control (i.e. without dietary supplement). The mean urinary fluoride level in the test group was found to decline progressively during the period of supplementation. The study revealed that consumption of amla powder may play an important role in mitigating fluoride-induced toxicity.

Keywords: Amla powder, ameliorating effect, dietary supplement, fluoride toxicity.

FLUORIDE, ingested through water and food accumulates in the human body and causes fluorosis. Fluoride may enter the body through sources other than drinking water, viz. (i) food and food products, spiced with black rock salt with 157 mg/l fluoride, (ii) use of fluoridated dental products, (iii) industrial emission of fluoride dust and fumes[1], and (iv) chewing supari and tobacco which have high fluoride content[2]. The maximum acceptable limit of fluoride in drinking water according to BIS[3] is 1.0 mg/l.

Bhupnagar village in the Amas Block of Gaya district, Bihar, is a fluoride endemic village, with mean F levels = 2.857 ± 0.11 mg/l. It was found that in this area, 47% of the entire fluoride intake for an adult was through drinking water followed by cereals and pulses (28%), and vegetables (25%)[4]. The residents of this village were found to suffer from dental, skeletal and non-skeletal fluorosis[5]. Anomalies were also found in the thyroid function[6] and haematological parameters[7] of the residents of Bhupnagar village.

As there are no medicines and/or surgical interventions to recover from fluorosis, the only alternatives are: (i) diet editing, where all sources of fluoride entry are withdrawn, and (ii) diet counselling for improving the health through consumption of essential nutrients and vitamins, antioxidants and micro nutrients. Vitamin C is one of the essential nutrients that would ameliorate fluorosis. Further, vitamin C enhances the absorption of nutrients by the gastrointestinal track[8].

Epidemiological studies in India[9] and Japan[10] suggest that the incidence and severity of fluorosis are related to the economic and nutritional status of the community. It

*For correspondence. (e-mail: shahla_apex@yahoo.co.in)